3

Towards the imaging of Weibel-Palade body biogenesis by Serial Block Face - Scanning Electron Microscopy

Journal of Microscopy, 2015, doi: 10.1111/jmi.12222

Marie J. Mourik
Frank G. A. Faas
Hans Zimmermann
Jeroen C. J. Eikenboom
Abraham J. Koster

3

Abstract

Electron microscopy is used in biological research to study the ultrastructure at high resolution to obtain information on specific cellular processes. Serial Block face Scanning Electron Microscopy (SBF-SEM) is a relatively novel electron microscopy imaging technique that allows three dimensional characterization of the ultra-structure in both tissues and cells by measuring volumes of 1000's of cubic micrometers yet at nm-scale resolution. In the scanning electron microscope (SEM), repeatedly an image is acquired followed by the removal of a thin layer resin embedded biological material by either a microtome or a Focused Ion Beam (FIB). In this way each recorded image contains novel structural information which can be used for three dimensional analysis.

Here, we explore FIB facilitated SBF-SEM to study the endothelial cell specific storage organelles, the Weibel-Palade bodies (WPBs), during their biogenesis at the Golgi apparatus. WPBs predominantly contain the coagulation protein Von Willebrand factor (VWF) which is secreted by the cell upon vascular damage. Using FIB facilitated SBF-SEM we show that the technique has the sensitivity to clearly reveal subcellular details like mitochondrial cristae and small vesicles with a diameter of about 50 *nm. Also we reveal numerous associations between WPBs and Golgi stacks which became conceivable in large scale three dimensional data. We demonstrate that SBF-SEM is a promising tool that offers an alternative for electron tomography to study subcellular organelle interactions in the context of a complete cell.*

3.1 Introduction

Microscopy on biological samples is a powerful tool to localize specific proteins or organelles to study their behavior, their morphological properties and their associations with other cell components. Transmission electron microscopy (TEM) can reveal cellular structures at the highest resolution but is often limited in showing 'the bigger picture' in the third dimension as the material has to be sectioned into 100 – 200 nm thick slices to allow imaging. Examining serial TEM sections in combination with the collection of serial electron tomograms can partially overcome this limitation.[1,2] However, both techniques are laborious and time consuming because of the required time for acquisition, processing and handling. Serial sectioning and serial electron tomography are therefore practically applicable for limited volumes in the order of 10's of cubic microns. Studies focusing on cell-cell contacts in tissue, or studies to characterize the three dimensional organization of subcellular organelles, are therefore not particularly suitable to be approached using TEM. A relatively novel way to study the relationships between cells or organelles is serial block face scanning electron microscopy (SBF-SEM).[3] In this imaging modality, the SEM images the block face of resin embedded material every time a microtome or Focused Ion Beam (FIB) has removed of a thin slice of material. As SBF-SEM can be performed automatically, large volumes of resin embedded material can be imaged which potentially can reveal novel features which stay unnoticed in 2D TEM sections. The differences between SBF-SEMs using an integrated microtome and those that use a FIB, are mainly related to the attainable slice thickness and to the surface area that is removed from the block: the microtome can section down to 25 – 200 nm and removes a slice from the entire block surface while the FIB operates locally on a selected area and can remove slices as thin as 3 nm.[3] Currently, SBF-SEM is a particular popular technique to image cell-cell interactions in tissues. Because of its technical capabilities we set out to explore whether the technique could also be effectively used to study subcellular organelles. In this paper we describe the application of SBF-SEM to study Weibel-Palade bodies (WPBs) in endothelial cells.[4]

WPBs are storage organelles found in endothelial cells. These cells line blood vessels and form a barrier between the blood and the underlying tissue.[4] The WPBs were serendipitously discovered by TEM and were described as rod or cigar shaped organelles of 0.1 – 0.3 μm in diameter and 1 – 5 μm in length. WPBs typically display densely packed tubules[4,5] which are formed by the hemostatic protein Von

Willebrand factor (VWF). VWF is secreted by endothelial cells upon vascular damage, inflammation or hypoxia and initiates the first steps in hemostasis.[5]

As endothelial cells have to respond on demand, a sufficient storage pool of WPBs is formed in advance. Biogenesis of WPBs occurs at the Golgi apparatus and is possibly induced by VWF itself. It has been shown that expression of full-length VWF in non-endothelial cells can result in the formation of so called 'pseudo-WPBs'.[6,7] However, recent data suggest that the Golgi is also heavily involved in controlling WPB content and WPB size.[8] Studying the morphology of forming WPBs by TEM is still providing novel information but is limited in providing the large scale three dimensional information as only thin sections of cells can be studied at once. Here, we explore FIB facilitated SBF-SEM to determine whether the technique provides the resolution and the sensitivity to study subcellular interactions such as WPB biogenesis at the Golgi apparatus.

3.2 Materials and methods

Cell culture

Human umbilical vein endothelial cells (HUVEC) obtained from Lonza (Walkersville, MD) were cultured in endothelial growth medium-2 (EGM-2 bulletkit, Lonza). Cell culture petri dishes and Thermanox™ coverslips (Thermo Scientific, Hudson, NH) were coated with 1% gelatin in PBS prior to cell seeding. Cells were grown for about 7 days till confluent.

Transmission electron microscopy

TEM samples were prepared as previously described.[9] Briefly, the cells were fixed in 2% glutaraldehyde in 0.1 M cacodylate buffer pH 7.4. Cells were post-fixed with 1% osmium tetroxide. Cells were dehydrated using a gradient series of ethanol and were embedded in Epon LX-112. The resin was polymerized for 48 hours at 60 °C. Ultra-thin sections of 100−120 nm thick were prepared and placed on copper EM grids. The sections were post stained with 7% uranyl acetate and Reynold's lead citrate. TEM images were acquired using a Tecnai 12 (FEI company, Eindhoven, The Netherlands) TEM at 120 kV equipped with an Eagle 4k×4k CCD camera (FEI company).

Focused ion beam - scanning electron microscopy

Samples for FIB-SEM imaging were prepared as previously described.[10] In short, cells were fixed for 1 hour in 1.5% glutaraldehyde in 0.1 M cacodylate buffer pH 7.4. Cells were placed on ice for 1 hour in 2% osmium tetroxide 1.5% potassium ferrocyanide in 0.1 M cacodylate bufer. A 1% thiocarbohydrazide solution was prepared fresh in water and filtered through a 0.22 μm Millipore syringe filter before use. It was placed on the cells for 20 minutes at room temperature. Then, the cells were incubated in 2% osmium tetroxide in water for 30 minutes. Cells were kept overnight in 1% aqueous uranyl acetate at 4 °C. Next day, Walton's lead aspartate was freshly prepared, filtered through a 0.2 μm Millipore syringe and placed on the cells for 30 minutes at 60 °C. Dehydration was performed using a series of ethanol incubations. The cells were then placed in ice-cold 100% anhydrous acetone. Durcupan AMC resin was infiltrated into the cells using 25, 50 and 75% Durcupan solutions in acetone. Cells were placed in 100% Durcupan resin overnight. Excess resin was removed and resin filled BEEM® capsules were placed on top of the cells. The resin was polymerized at 60 °C for 48-72 hours.

The polymerized resin capsules were removed from the coverslips. The monolayer of cells is retained on the surface of the resin block. A 1 mm slice was cut from the resin block using a saw. The block was placed on a SEM stub using carbon tape. Silver paint was applied on the sides of the block to electrically ground the sample. Additionally, a thin layer of iridium was sputtered on top of samples using an Emitech K575X coater (Quorum Technologies Ltd, Laughton, United Kingdom).

Imaging was performed using an Auriga CrossBeam (Carl Zeiss Microscopy GmbH, Munich, Germany) SEM at an acceleration voltage of 1.7 kV using an image aperture of 30 μm(high current; beam current: $\sim$ 220 pA). The signals from the InLens secondary electron detector and the energy selected backscattered (EsB) electron detector were mixed because it provided the best signal to noise ratio. The grid voltage of the EsB detector was set at 1108 V. After every acquired image, a 10 nm slice was removed using the FIB. A milling current of 4 nA was used at an acceleration voltage of 30 kV.

Image processing and visualization

To refine the alignment of the image stack as produced by the instrument, first the support layer was localized within each image. Next, the images were pair-

wise aligned by weighted phase correlation. The Gaussian weight window was set at an offset to the support layer and the tapering was chosen such that the 3-sigma boundary was well within the cell monolayer. The pairwise shift was determined by a parabolic fit centered around the location of maximum correlation value. All image processing was implemented using MATLAB® and the DIPimage toolbox.[11] Segmentation of subcellular structures in the aligned image stack was performed in Amira® (Visualization Sciences Group, FEI). To load the data set, the images were cropped and binned two times in x and y. The structures were segmented by using the threshold option on selected regions or by manual drawing. Additionally, the segmented volumes were smoothened.

3.3 Results

Serial Block Face - SEM on a single cell layer reveals most of the major cell structures

To explore whether we could use SBF-SEM for the analysis of WPBs forming at the Golgi apparatus we first wanted to establish to which extend details can be resolved by SEM in chemically fixed cells. Performing SBF-SEM on single cell layers can be more challenging as the underlying resin has the tendency to charge by the lack of conducting material. We experienced that the level of detail required for the identification of WPB was best imaged with a SBF-SEM system that uses a FIB to remove material. In a FIB-SEM system, the sample is tilted in the SEM chamber to alternately image the sample from the top by SEM, and mill material away with the FIB from the side (Figure 3.1A). To open up the material and to start subsequent imaging and FIB milling, a trench has to be milled by the FIB (Figure 3.1A and B). As shown in Figure 3.1B, the HUVECs appeared as a very thin line just beneath the resin block surface. When zooming in on the exposed cells, many intracellular organelles were clearly revealed when acquiring several image stacks. Apart from the nucleus, we most often observed the abundant membrane stacks of the Golgi apparatus (Figure 3.2A), the wide spreading network of the endoplasmic reticulum (Figure 3.2B), the lysosomes (Figure 3.2B) and the mitochondria (Figure 3.2C). As shown in Figure 3.2C, the internal cristae within the mitochondria were clearly visible. In addition to this, we could also distinguish centrosomes (Figure 3.2D-D'), occasional microtubules (arrowheads Figure 3.2E) and caveolae (arrowheads Figure 3.2F) which are tiny 50 to 100 nm vesicles that are formed at the plasma membrane of endothelial cells for transcytosis. Common

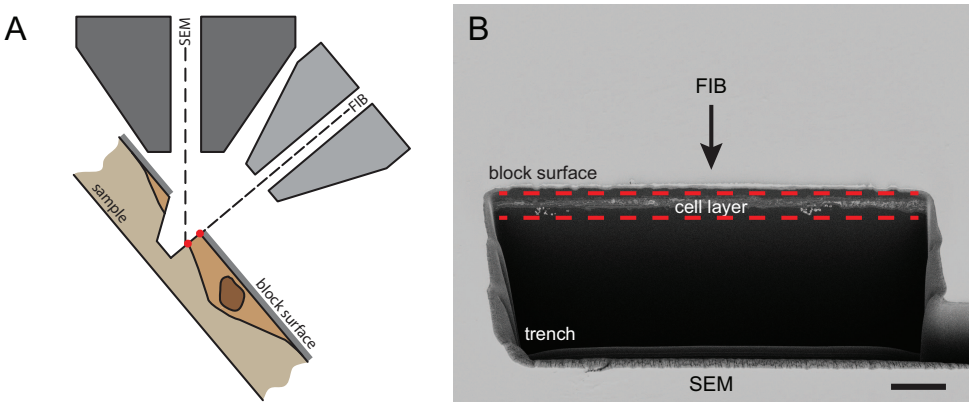

Figure 3.1. Focused Ion Beam milling for Serial Block Face-SEM.(Overview of the imaging setup and the sample. (A) Schematic representation showing the beam line of the electrons of the Scanning Electron Microscope (SEM) and the ions of the Focused Ion Beam (FIB) with respect to the sample. The sample is tilted such that the electron beam can image from the top while the FIB can remove material from the side. A trench is created by the FIB to make the sample accessible for SBF imaging. (B) Low magnification overview imaged by the SEM showing the trench created for SBF-SEM imaging. Between the dashed lines the monolayer of cell material is observed. Scale bar is 5 μm.

cellular structures that were not detected in the SBF-SEM stacks were mainly fine proteinaceous components such as actin filaments, clathrin coats and ribosomes. Because of the severe fixation and staining procedure that was used to prepare the specimen for SBF-SEM imaging some of these structures may be perturbed and not be visible.

Weibel-Palade body imaging by Serial Block Face-SEM

In our search to WPBs in the acquired image stacks we experienced that longitudinally sectioned WPBs were observed less frequently. Further analysis of the data indicated that most WPBs were visualized in a cross sectional orientation (Figure 3.3A). The elongated shape of these WPBs was revealed when visualizing the three dimensional volume in a different orientation and upon segmentation (supplemental Video 1).

When observed by TEM, the internal structure of longitudinally sectioned WPB typically reveals striations of VWF tubules (Figure 3.3B). However, when we examined WPBs in the SEM data the tubules were hardly resolved and appeared as a uniformly stained mass as shown in the inverted SEM image depicted

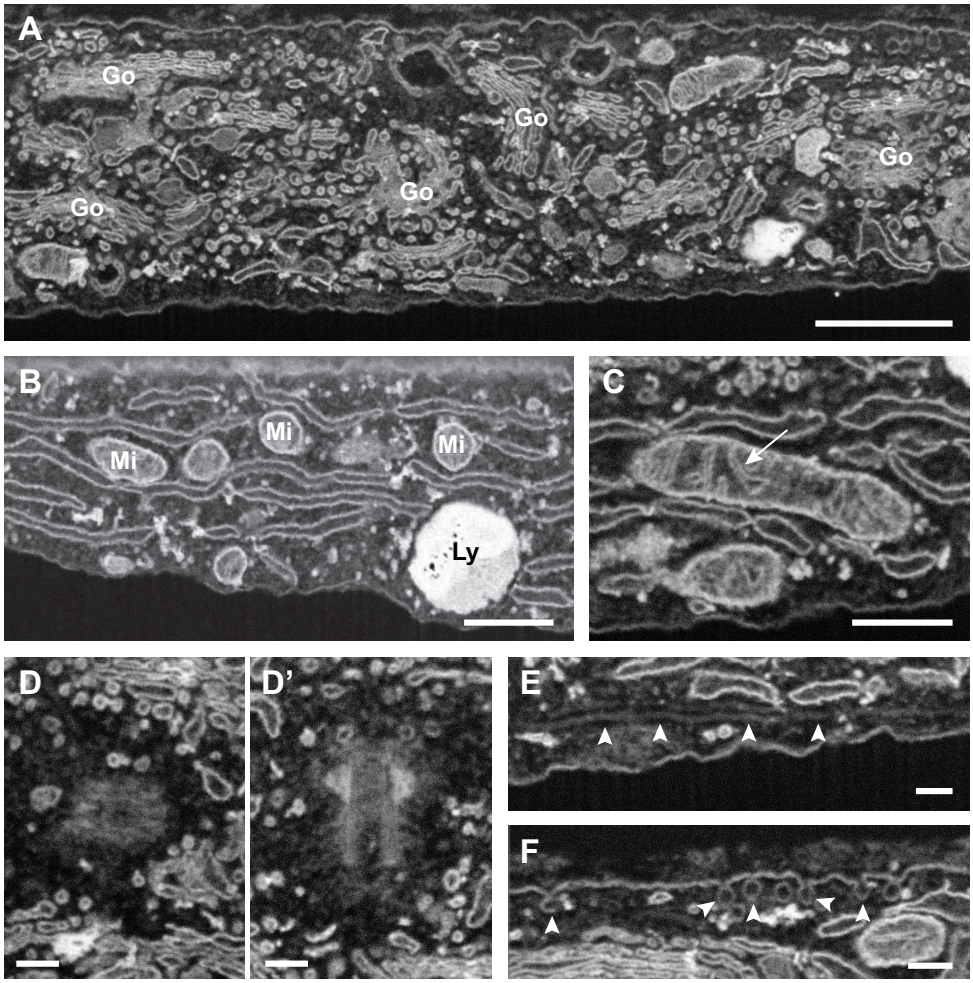

Figure 3.2. Organelles and subcellular structures by Serial Block Face-SEM.(Overview of the subcellular structures and cell organelles in endothelial cells observed by SBF-SEM. (A) The extensive membrane stacks of the Golgi apparatus (Go). (B) Membrane network of the Endoplasmic Reticulum. In addition also a lysosome (Ly) and parts of mitochondria (Mi) are observed. (C) Mitochondrion in which the internal cristae are clearly resolved (arrow). (D-D') Pair of centrosomes. (D) Centrosome from the top. (D') Centrosome from the side. (E) Microtubule (arrowheads) running just beneath the plasma membrane. (F) Caveolae at the plasma membrane. Scale bar panel A is 1 μm. Scale bar panel B and C is 500 nm. Scale bar panels D-F is 200 nm.

in (Figure 3.3C). Revealing the VWF tubules is essential to study WPB formation and maturation as the size and the amount of tubules provides information on the advancement of the WPB during its biogenesis. As shown in Figure 3.3D, TEM on immature WPBs near the membranes of the Golgi apparatus clearly reveals the initial loose packaging of the VWF tubules. During the formation process, these immature WPBs will further increase in size and are finally condensed to create tightly packed mature WPBs. The WPBs observed around the Golgi stacks by SBF-SEM appeared, similar to those imaged by TEM, less electron dense but unfortunately did not reveal the VWF tubules (Figure 3.3E). A more tailored approach to the image acquisition as well as in sample preparation will probably be required to resolve such kind of detail.

Analysis of the Golgi apparatus and surrounding Weibel-Palade bodies reveals close relationships

To obtain insight into the cellular spatial organization of forming WPBs around the Golgi, a stack of almost 1600 images was collected at 25000×magnification. We imaged an area of about 11.4 μm by 8.5 μm with a milling thickness of 10 nm which resulted in a voxel resolution of 3.7×3.7×10 nm. In total a volume of about 16 microns depth was imaged and removed from the block surface in a timespan of approximately 50 hours which corresponds to an acquisition speed of about 32 images per hour. This was achieved using a FIB milling time of about 2 seconds and a SEM acquisition time of about 2 minutes per image. To analyze and segment the volume in Amira®, the dataset was aligned by phase correlation with a Gaussian window function. In addition the data was cropped and binned two times in x and y.

Figure 3.4A shows a three dimensional representation of the imaged volume containing cellular material. In this volume we segmented the Golgi and the WPBs (Figure 3.4B-C and supplementary Video 2) to reveal the distribution of the Golgi as well as its associations with WPBs. In addition we also modeled the nucleus and cell membrane to show the Golgi and WPBs in the context of the cell. From the model we can observe that the WPBs that are in close proximity to a Golgi stack appear to concentrate in some specific region. Several of these WPBs even reveal tight associations and possible connections with Golgi stacks (WPBs are indicated in red in Figure 3.4B and C, see also supplementary Video 2). Interestingly most of the modeled WPBs are already of remarkable size suggesting that advanced immature WPBs remain associated with the Golgi membrane. In addition, the seg-

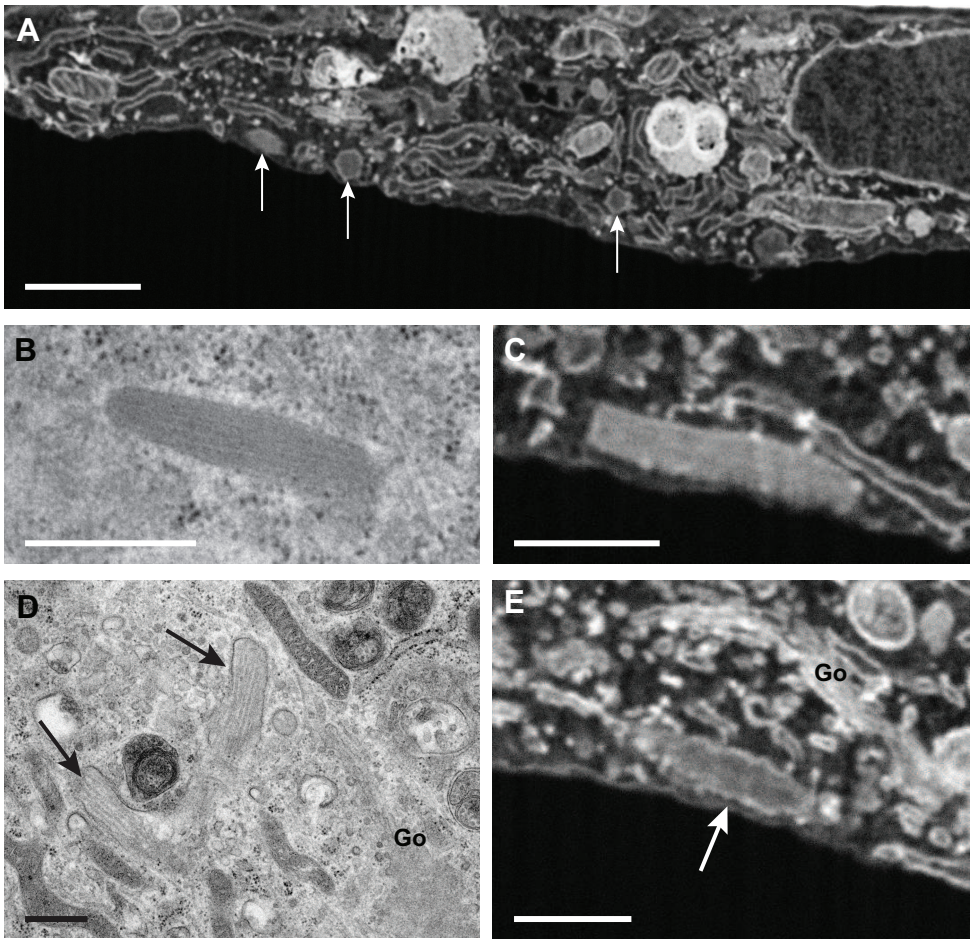

Figure 3.3. Weibel-Palade bodies imaged by SEM and TEM(Weibel-Palade bodies (WPBs) imaged by SEM and TEM in endothelial cells. (A) SBF-SEM slice showing cross sectioned WPBs (arrows). See also supplementary Video 1. (B) Longitudinal sectioned WPB imaged by TEM displaying internal striations of Von Willebrand factor tubules.(C) Inverted SEM image of a longitudinal sectioned WPB that displays a uniform stained interior.(D) Immature WPBs (arrows) near the Golgi apparatus (Go) imaged by TEM. Separate VWF tubules are clearly visible. (E) Inverted SEM image of an immature WPB near the Golgi apparatus (Go). Interior is less electron dense than the WPB in panel C but the VWF tubules are not resolved. Scale bar panel A is 1 μm. Scale bar panels B-E is 500 nm.

mentation of the cell membrane emphasizes the flatness of the endothelial cell, a characteristic that is often overlooked and underestimated when flat-embedded endothelial cells are studied by conventional TEM.

3.4 Discussion

SBF-SEM is an effective method to study the 3D organization of subcellular structures. We show that this technique clearly resolves the general cell components at a resolution level that shows details at the level of mitochondrial cristae and vesicles of about 50 nm in diameter. In addition, we could recognize the endothelial specific storage organelles, the WPBs, and reveal their organization around the Golgi apparatus. Interestingly, the WPBs that were in close proximity to the Golgi seemed to cluster at specific region. Moreover, close associations between Golgi apparatus membranes and WPBs were observed that are exciting to study in further detail, especially because large WPBs were observed as well. This could suggest that the WPBs are fully formed at the Golgi.

When we compared the morphology of the WPBs that were observed by SEM to electron micrographs of WPBs imaged by TEM we observed that the characteristic tubular interior of the WPB was not visible in the SEM data. We speculate that these tubular structures were difficult to image by the SEM due the severe fixation and staining method. In addition, the limited depth in which the electrons interact with the stained material in the resin block and the limited sensitivity of the used detectors may also have influenced the image quality. Most of the currently available staining methods were largely designed to study neuronal networks in brain tissue and are therefore mainly focusing on intense membrane staining.[10,12] To reveal the VWF tubules, a different staining protocol could be needed to preserve and highlight these structures as well. Another improvement can be expected by the application of high pressure freezing and freeze substitution as they improve the ultra-structural preservation of the WPBs and VWF tubules.[13] To date only a few freeze substitution protocols have been published for SBF-SEM.[14,15]

A critical point for imaging single cell layers is the conductivity of the sample. Single cell layers tend to charge faster than blocks of embedded tissue due to the high resin content that lacks conductive material that is formed by the metals staining cellular structures. Charging of the resin block leads to image deformation and image shifts which hamper automated data collection of large volumes

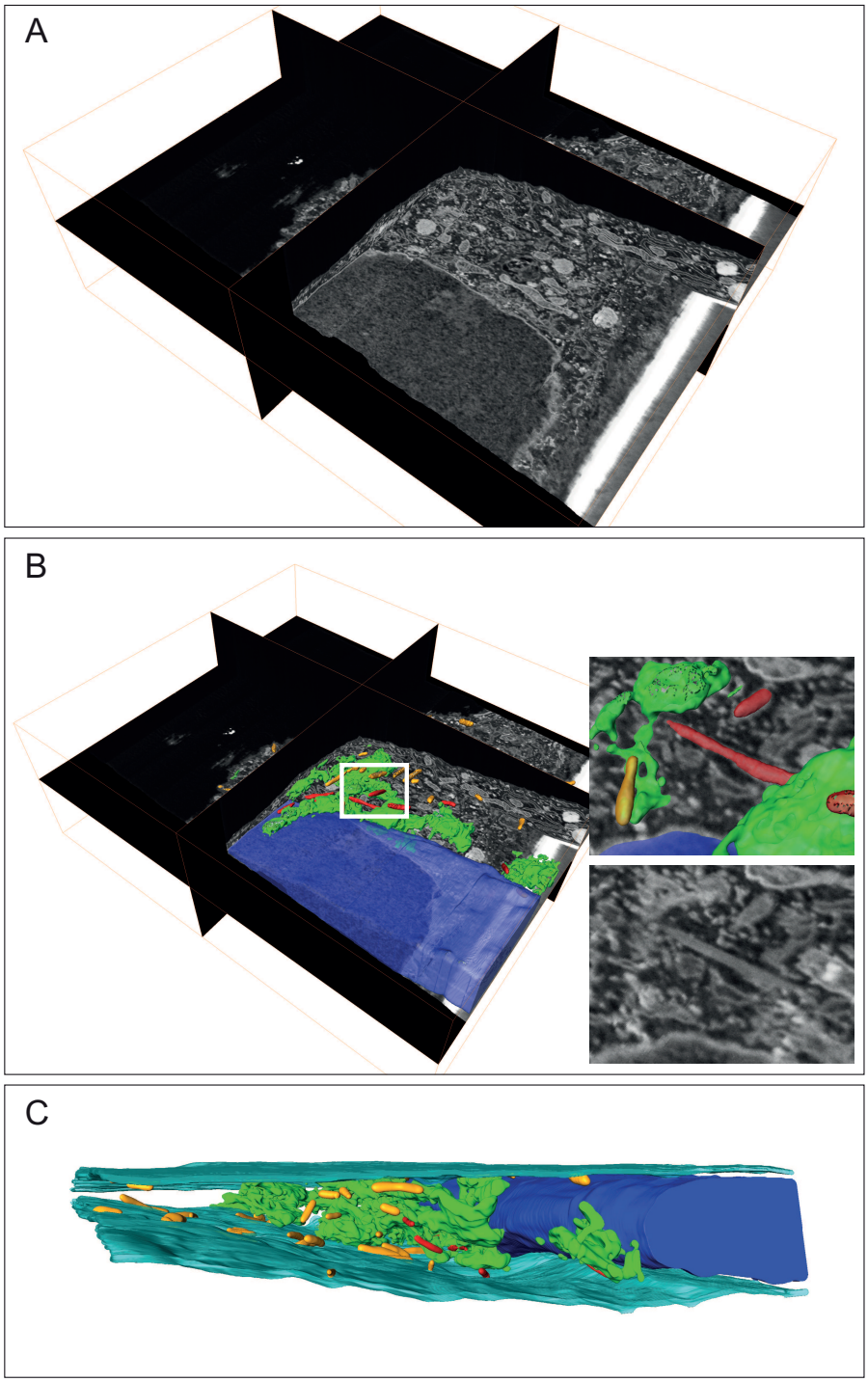
A
B
C

Figure 3.4. Serial Block Face-SEM reveals Weibel-Palade bodies in close association with the Golgi. Analysis and modelling of a large SBF-SEM stack to study WPBs in relation to the Golgi apparatus in endothelial cells. (A) Three dimensional overview of the dataset. The dataset consist of almost 1600 images and was acquired at 25000× magnification using a 10 nm slice thickness. For processing the data was binned 2 times in x and y which resulted in a voxel resolution of 7.4 × 7.4 × 10 nm. (B) Segmentation of the volume reveals the large size of the Golgi apparatus (green) and the WPBs (red) that are in close association with the Golgi. In addition, we segmented the peripheral WPBs (yellow) and the nucleus (blue). The inserts show one of the WPBs that was found in close relationship with the Golgi. Scale bar is 500 nm. To have a better view on the ultrastructure the data was rotated with respect to the orientation in which the data was acquired for panels A and B. (C) Segmentation of the cell membrane additionally reveals the confined and flat morphology of the endothelial cell. Scale bar is 1 μm.

and will lead to inaccurate alignment of the data. We observed significant variation between samples which were prepared similarly. Some of the samples were stable during the FIB milling and subsequent SEM imaging while others were a challenge to image because of apparent charging which was visible in image deformation and image shifts. We experienced that leaving the sample under vacuum for several days as well as applying an additional iridium coat on the block surface reduced charging effects. Mixing currently available resins with cell-impermeable conductive material may solve the charging issues and could be beneficial for SBF-SEM imaging of single cell layers. However, this possibility has not been explored so far.

In spite of the occasional charging issue, the obtained image quality using the available sample preparation methods combined with high-end SEMs is a revolutionary step forward in the capabilities of electron microscopy to image cells and tissue 1000's of cubic micrometers in size yet at 5 − 20 nm resolution. Acquired SEM images as presented here, are to a large extend similar to TEM, revealing detailed structures such as the mitochondrial cristae and small 50 nm vesicles. In addition, it has been shown that FIB milling can remove slices up to 3 nm from the block surface. This demonstrates that SBF-SEM can offer for many cases a good alternative for electron tomography.[16] A major advantage is that FIB facilitated SBF-SEM can image large volumes in a single data collection session which saves time when compared to electron tomography on serial sections. A second advantage compared to serial section electron tomography is that a continuous image stack can be acquired and that no information is lost during sectioning as is often seen in serial TEM sections. On the down side, SBF-SEM does not yet reveal

the extent of details as resolved by electron tomography. For example, electron tomography easily reveals individual tubules of VWF in WPBs.[9]

To localize specific areas of interest for SBF-SEM imaging, Correlative Light and Electron Microscopy (CLEM) could beneficial. With CLEM, light microscopy is used to localize and map the fluorescently stained structures of interest in a biological sample for subsequent investigation by EM in order to reveal the morphological and structural characteristics.[17] Currently several groups have shown the power of CLEM and SBF-SEM in tissue and cells.[18–20] However, to perform CLEM to localize subcellular structures in 3D by SBF-SEM some challenges have to be met. CLEM on subcellular structures depends much more on the accuracy of the overlay between the fluorescence data and the SBF-SEM stack when compared to CLEM aiming to relocate a single cell in tissue. As also shown by Murphy et al.[19], the fluorescent images are most often acquired in a different orientation than the orientation used to obtain the SBF-SEM stack. Therefore much more advanced image processing is required to overlay the two data sets.[19] The use of bi-modal fiducials that are visible in both imaging modalities may therefore be used to obtain an accurate overlay. For monolayers for example, bi-modal fiducials could be applied underneath the cells prior to cell seeding and on top to the cell prior to fluorescence microscopy. Also novel image processing tools are required that can overlay and display the two correlated data sets in a suitable way for analysis and annotation.

In our journey to explore SBF-SEM for the imaging of WPBs, we experienced that SBF-SEM is a suitable tool to further investigate the more detailed morphological characteristics of the WPBs formation at the Golgi apparatus. To optimally use SBF-SEM for this purpose, optimization of the fixation and staining protocol is needed to elucidate the VWF tubules as well. So far we were able to show the WPB distribution around the Golgi in a large three dimensional volume. In addition we could reveal that some of these WPBs were in close proximity or even connected to the Golgi membrane. Apart from WPB biogenesis, SBF-SEM will also be an effective approach to study the three dimensional organization upon WPB exocytosis. However, to efficiently study these biological processes in a targeted way the combination with a CLEM method will be needed to pinpoint the structures of interest using fluorescence.

3.5 Acknowledgments

The authors would like to thank Roman Koning for help with Amira. This work was financially supported by the Netherlands Organization for Scientific Research (NWO TOP, grant no. 91209006).

References

[1] B. K. Hoffpauir, B. A. Pope, and G. A. Spirou, *Serial sectioning and electron microscopy of large tissue volumes for 3d analysis and reconstruction: a case study of the calyx of held,* Nat Protoc **2**, 9 (2007).

[2] M. Barcena and A. J. Koster, *Electron tomography in life science,* Semin Cell Dev Biol **20**, 920 (2009).

[3] G. Knott and C. Genoud, *Is em dead?* J Cell Sci **126**, 4545 (2013).

[4] E. R. Weibel and G. E. Palade, *New cytoplasmic components in arterial endothelia,* J Cell Biol **23**, 101 (1964).

[5] K. M. Valentijn, J. E. Sadler, J. A. Valentijn, J. Voorberg, and J. Eikenboom, *Functional architecture of weibel-palade bodies,* Blood **117**, 5033 (2011).

[6] J. Voorberg, R. Fontijn, J. Calafat, H. Janssen, J. A. van Mourik, and H. Pannekoek, *Biogenesis of von willebrand factor-containing organelles in heterologous transfected cv-1 cells,* EMBO J **12**, 749 (1993).

[7] G. Michaux, L. J. Hewlett, S. L. Messenger, A. C. Goodeve, I. R. Peake, M. E. Daly, and D. F. Cutler, *Analysis of intracellular storage and regulated secretion of 3 von willebrand disease-causing variants of von willebrand factor,* Blood **102**, 2452 (2003).

[8] F. Ferraro, J. Kriston-Vizi, D. J. Metcalf, B. Martin-Martin, J. Freeman, J. J. Burden, D. Westmoreland, C. E. Dyer, A. E. Knight, R. Ketteler, and D. F. Cutler, *A two-tier golgi-based control of organelle size underpins the functional plasticity of endothelial cells,* Dev Cell **29**, 292 (2014).

[9] K. M. Valentijn, J. A. Valentijn, K. A. Jansen, and A. J. Koster, *A new look at weibel-palade body structure in endothelial cells using electron tomography,* J Struct Biol **161**, 447 (2008).

[10] P. S. Holcomb, B. K. Hoffpauir, M. C. Hoyson, D. R. Jackson, T. J. Deerinck, G. S. Marrs, M. Dehoff, J. Wu, M. H. Ellisman, and G. A. Spirou, *Synaptic inputs compete during rapid formation of the calyx of held: a new model system for neural development,* J Neurosci **33**, 12954 (2013).

[11] C. L. Hendriks, L. Van Vliet, B. Rieger, G. van Kempen, and M. van Ginkel, *Dipimage: a scientific image processing toolbox for matlab,* Quantitative Imaging Group, Faculty of Applied Sciences, Delft University of Technology, Delft, The Netherlands (1999).

[12] J. C. Tapia, N. Kasthuri, K. J. Hayworth, R. Schalek, J. W. Lichtman, S. J. Smith, and J. Buchanan, *High-contrast en bloc staining of neuronal tissue for field emission scanning electron microscopy,* Nat Protoc **7**, 193 (2012).

[13] H. L. Zenner, L. M. Collinson, G. Michaux, and D. F. Cutler, *High-pressure freezing provides insights into weibel-palade body biogenesis,* J Cell Sci **120**, 2117 (2007).

[14] D. H. Hall, E. Hartwieg, and K. C. Nguyen, *Modern electron microscopy methods for c. elegans,* Methods Cell Biol **107**, 93 (2012).

[15] C. Villinger, H. Gregorius, C. Kranz, K. Hohn, C. Munzberg, G. von Wichert, B. Mizaikoff, G. Wanner, and P. Walther, *Fib/sem tomography with tem-like resolution for 3d imaging of high-pressure frozen cells,* Histochem Cell Biol **138**, 549 (2012).

[16] K. Narayan, C. M. Danielson, K. Lagarec, B. C. Lowekamp, P. Coffman, A. Laquerre, M. W. Phaneuf, T. J. Hope, and S. Subramaniam, *Multi-resolution correlative focused ion beam scanning electron microscopy: Applications to cell biology,* J Struct Biol (2013), 10.1016/j.jsb.2013.11.008.

[17] A. A. Mironov and G. V. Beznoussenko, *Correlative light-electron microscopy a potent tool for the imaging of rare or unique cellular and tissue events and structures,* Methods Enzymol **504**, 201 (2012).

[18] H. E. Armer, G. Mariggi, K. M. Png, C. Genoud, A. G. Monteith, A. J. Bushby, H. Gerhardt, and L. M. Collinson, *Imaging transient blood vessel fusion events in zebrafish by correlative volume electron microscopy,* PLoS One **4**, e7716 (2009).

[19] G. E. Murphy, K. Narayan, B. C. Lowekamp, L. M. Hartnell, J. A. Heymann, J. Fu, and S. Subramaniam, *Correlative 3d imaging of whole mammalian cells with light and electron microscopy,* J Struct Biol **176**, 268 (2011).

[20] M. S. Lucas, M. Guenthert, P. Gasser, F. Lucas, and R. Wepf, *Correlative 3d imaging: Clsm and fib-sem tomography using high-pressure frozen, freeze-substituted biological samples,* Methods Mol Biol **1117**, 593 (2014).

3.A Supplementary material

Video 1.

3D visualization of cross sectioned Weibel-Palade bodies in endothelial cells. The dataset was acquired at 25000× magnification using a 10 nm slice thickness. For processing the data was binned 2 times in x and y which resulted in a voxel resolution of 7.4 × 7.4× 10 nm.

https://www.dropbox.com/s/h33miyy1pb1jn6n/ChIII_Video1.mov?dl=0

Video 2.

3D Visualization of the Golgi apparatus with associating Weibel-Palade bodies in endothelial cells. The dataset consist of almost 1600 images and was acquired at 25000× magnification using a 10 nm slice thickness. For processing the data was binned 2 times in x and y which resulted in a voxel resolution of 7.4×7.4× 10 nm.

https://www.dropbox.com/s/yosd2ux2kwqqj64/ChIII_Video2.mov?dl=0